New Approach to Finite-State Modeling of Unsteady Aerodynamics

C. Venkatesan* and P. P. Friedmann†
University of California, Los Angeles, California

A novel technique used in control engineering for formulating a high-quality, finite-state, unsteady aerodynamic model by applying Bode plot methods is presented. Indicial response functions for both fixed- and rotary-wing applications are obtained using these finite-state, unsteady aerodynamic models. It is shown that the rotary-wing indicial response function has a fundamentally different characteristics when compared to fixed-wing indicial response. The rotary-wing indicial response function is oscillatory in nature, while the fixed-wing indicial response function is nonoscillatory. Furthermore, it should be emphasized that this is the first literary presentation of rotary-wing indicial response function.

Nomenclature

a	= lift-curve slope
a_i, b_i	= coefficients in approximate aerodynamic transfer function
b	= blade semichord
$C(k)$	= Theodorsen's lift deficiency function
$C(\bar{s})$	= generalized Theodorsen's lift deficiency function
C'	= Loewy's lift deficiency function
C_T	= thrust coefficient
F,G	= real and imaginary parts of Theodorsen's lift deficiency function, $C=F+iG$
F',G'	= real and imaginary parts of Loewy's lift deficiency function, $C=F'+iG'$
$G(i\omega)$	= transfer function
$H_n^2(k)$	= Hankel functions of second kind of order n; $H_n^2=J_n-iY_n$
$\bar{h}_e$	= equivalent wake spacing, $=2\pi U_{p0}/Q\Omega b$
$J_n(k)$	= Bessel functions of first kind of order n
$K_n(\bar{s})$	= modified Bessel functions of second kind of order n
k	= reduced frequency, $=\omega b/\Omega r$ or $\omega b/U$
L	= lift per unit span of the blade
L_c	= circulatory lift on the airfoil
$\bar{m}_e$	= equivalent frequency ratio, $=\omega/\Omega Q$
Q	= number of blades in a rotor or ¾-chord downwash velocity
R	= rotor radius
$\bar{r}_e$	= radial station for the typical blade section, r/bQ
s	= Laplace variable
$\bar{s},\tilde{s}$	= nondimensional Laplace variables; $\bar{s}=bs/\Omega 0.75R$, $\bar{s}=s/\Omega$, $\tilde{s}=(b/U)s$
U	= freestream velocity
U_{p0}	= induced velocity normal to the rotor
ρ	= density of air
τ	= nondimensional time, $(0.75R/b)\Omega t$
$\phi_{FW}(\tau),\phi_{RW}(\tau)$	= fixed- and rotary-wing indicial response functions, respectively
Ω	= rotor rpm
ω	= frequency

Received Aug. 27, 1985; revision received April 30, 1986.

*Assistant Research Engineer, Mechanical, Aerospace, and Nuclear Engineering Department.

†Professor of Engineering and Applied Science. Associate Fellow AIAA.

Introduction

IT is well known that the role of unsteady aerodynamics is important for aeroelastic stability and response calculations in both rotary- and fixed-wing applications. A wide array of mathematical models has been developed to represent unsteady aerodynamic loads, starting from simple and computationally efficient models and culminating in very complicated, computationally expensive models capable of capturing the intricate details of unsteady flow. Two-dimensional, unsteady aerodynamic theories, which provide analytic expressions for the unsteady loads on a moving airfoil, are usually based on the assumption of simple harmonic motion of the airfoil. Representative theories in this category are: 1) Theodorsen's[1] incompressible, two-dimensional, unsteady aerodynamic theory and Greenberg's[2] extension of Theodorsen's theory, which accounts for pulsating oncoming flow velocity and constant angle of attack; these theories have been developed for fixed wings, however, they have been frequently used in rotary-wing applications, and 2) Loewy's[3] and Shipman and Wood's[4] theories, which are applicable to a helicopter rotor in hover and forward flight, respectively.

The fundamental difference between the rotary- and fixed-wing unsteady aerodynamic theories lies in the modeling of unsteady wakes due to the airfoil motion. Theodorsen's theory, for fixed-wing cases, assumes a planar wake behind the airfoil extending to infinity; whereas Lowey's theory, for rotary wings, assumes an unsteady wake behind and beneath the reference airfoil extending to infinity in both directions (Fig. 1). These theories have a significant deficiency when applied to aeroelastic stability calculations, since the assumption of simple harmonic motion, upon which they are based, implies that they are strictly valid only at the stability boundary, and thus provide no information on system damping before or after the flutter condition is reached. Thus a standard stability analysis, such as the root locus method, cannot be used in conjunction with these theories. Furthermore, these unsteady aerodynamic theories are not suitable for the analyses of aeroelastic system with active controls—such as higher harmonic control devices—and the transient response analysis of aeroelastic system—such as rotor-blade response in forward flight. Thus, there is a need for unsteady aerodynamic theories capable of modeling unsteady aerodynamic loads, in the time domain for finite-time arbitrary motion of an airfoil, representing the cross section of an oscillating helicopter rotor blade. (In this paper, "arbitrary motion" is used to denote growing or decaying oscillations with a certain frequency.) For finite-time arbitrary motion of the airfoil, such an unsteady aerodynamic theory has been developed recently for fixed-wing applications. However, the success in developing similar theories suitable for rotary-wing applications has been limited.

A brief summary of the developments in finite-time, unsteady aerodynamic modeling for fixed-wing applications is presented for convenience. In the early 1940s, Laplace transform methods were applied to the problem of unsteady aerodynamics for finite-time arbitrary motion of an airfoil.[5-7] However, certain computational difficulties were encountered in extending these theories to values of the Laplace transform variable along the imaginary axis, which represents simple harmonic motion. Recently, Edwards[8] resolved the computational difficulties encountered in the application of the Laplace transform technique to the unsteady aerodynamics of a two-dimensional airfoil oscillating in incompressible flow. He showed that the Laplace transform of the circulatory load on the airfoil, executing arbitrary motion, is related to the product of the Laplace transform of the generalized Theodorsen function $C(\bar{s})$ and the Laplace transform of the ¾-chord downwash velocity of the airfoil. In the Laplace domain, the generalized Theodorsen lift deficiency function $C(\bar{s})$ is the same as replacing ik in Theodorsen's lift deficiency function $C(k)$ by the nondimensional Laplace transform variable $\bar{s}$.

Recently, Vepa[9] derived an approximate functional form for the aerodynamic transfer function corresponding to Theodorsen's lift deficiency function in terms of Padé approximants. Knowing the exact lift deficiency function $C(k)$, Vepa[9] represented $C(k)$ by the ratio of polynomials $N(ik)/D(ik)$, where $N(ik)$ and $D(ik)$ are equal-degree polynomials. Vepa evaluated the coefficients of the various terms of the polynomials by a least-squares technique and obtained a very good approximation to $C(k)$. Dowell[10] proposed a different procedure for obtaining the approximate expression for $C(k)$. His approach uses a parameter identification technique, in which the time history of the aerodynamic load on the airfoil was assumed to consist of sums of exponentials. Applying the fundamental correspondence between the frequency and time-domain aerodynamic loads, Dowell evaluated the time constants and the coefficients, which provide the best fit to the frequency domain representation of the aerodynamic forces. The approximate representations of Theodorsen's lift deficiency function $C(k)$, obtained by Vepa and Dowell, can be used to model the unsteady aerodynamic loads produced by completely arbitrary, small, time-dependent airfoil motions. Since these approximate transfer functions for $C(k)$ are finite-degree polynomials, they are also referred to as finite-state models for the unsteady aerodynamics.

A brief summary of rotary-wing-type unsteady aerodynamic theories is provided next. Loewy[3] was the first to present a closed-form solution for the unsteady aerodynamic loads acting on the cross section of a rotor blade performing simple harmonic oscillations in incompressible flow. The wake model assumed by Loewy is shown in Fig. 1. Loewy's unsteady aerodynamic theory is the rotary-wing counterpart of Theodorsen's theory for fixed wings. A clear description of Loewy's theory can be found in Ref. 11. The first attempt to generalize Loewy's theory for arbitrary motions was undertaken by Dinyavari and Friedmann.[12] In Ref. 12, Loewy's lift deficiency function C' was generalized by replacing ik in the lift deficiency function by the nondimensional Laplace operator $\bar{s}$. Following Dowell's procedure,[10] a finite-state Padé approximation to Loewy's lift deficiency was obtained. However, the approximate model obtained in this fashion was incapable of capturing the oscillatory behavior of Loewy's lift deficiency function.[12] This was a serious shortcoming because the oscillatory nature of Loewy's lift deficiency function is a unique characteristic of the unsteady aerodynamic loads acting on rotating blades.

The primary objectives of this paper are to: 1) present a novel technique for formulating a high-quality, finite-state, unsteady aerodynamic model suitable for both fixed- and rotary-wing applications by using Bode plot methods employed in control theory, 2) apply this technique to the formulation of the unsteady aerodynamic transfer function for Theodorsen's theory and a rotary-wing unsteady theory, such as Loewy's theory, for an airfoil undergoing arbitrary motion in the time domain, and 3) use the technique to formulate a rotary-wing-type indicial response function and compare it to its fixed-wing counterpart.

First, a novel technique for identifying and formulating the mathematical form of the finite-state, unsteady aerodynamic transfer function is presented. This technique is based upon the Bode plot method[13] used in control systems engineering. Subsequently, the finite-state, unsteady aerodynamic models are used to obtain indicial response functions for both rotary- and fixed-wing applications. It is shown that the rotary-wing indicial response functions are qualitatively different in nature when compared to its fixed-wing conterpart. For fixed wings, the indicial response function exhibits a steady exponential decaying form, for rotary wings, the indicial response function has an oscillatory form with exponential decay. Therefore, the rotary-wing indicial response overshoots the steady value at certain specific times. This feature of the rotary-wing indicial function has also been observed experimentally.[14]

Finite-State Modeling of Unsteady Aerodynamics

General Overview

In the derivation of unsteady aerodynamic load on a two-dimensional airfoil in incompressible flow, for finite-time arbitrary motion, Edwards[8] has shown that the generalized Theodorsen's lift deficiency function $C(\bar{s})$, obtained for arbitrary motion of the airfoil, can be expressed as

$$C(\bar{s}) = \frac{K_1(\bar{s})}{K_0(\bar{s}) + K_1(\bar{s})} \tag{1}$$

The circulatory portion of the lift per unit span of the airfoil in the Laplace domain can be written as

$$L_c(\bar{s}) = a\rho bUC(\bar{s})Q(\bar{s}) \tag{2}$$

where $Q(\bar{s})$ represents the Laplace transform of the ¾-chord downwash velocity.

For harmonic airfoil motion, the generalized Theodorsen lift deficiency function is obtained by replacing $\bar{s}$ by ik in Eq. (1), i.e.,

$$C(k) = \frac{H_1^2(k)}{H_1^2(k) + iH_0^2(k)} = F + iG \tag{3}$$

Since $C(k)$ given in Eq. (3) is known exactly, Vepa[9] constructed a Padé approximant for $C(k)$ by assuming

$$C(k) = F + iG \simeq \frac{N(ik)}{D(ik)} \tag{4}$$

where $N(ik)$ and $D(ik)$ are polynomials of equal degrees.

$$N(ik) = (ik)^n + a_1(ik)^{n-1} + \ldots + a_n \tag{5}$$

$$D(ik) = (ik)^n + b_1(ik)^{n-1} + \ldots + b_n \tag{6}$$

For nth-degree polynomials, the approximation is referred to as an $[n,n]$ Padé approximant. The coefficients $a_1,\ldots,a_n$ and $b_1,\ldots,b_n$ can be evaluated by minimizing the error

$$\sum_{j=1}^{m} \left[C(k_j) - \frac{N(ik_j)}{D(ik_j)} \right]^2$$

where $j = 1,\ldots,m$ refers to the value of k at selected m points. Using a fourth-degree polynomial for N and D; i.e., a [4,4] Padé approximation, Vepa evaluated the coefficients a and b

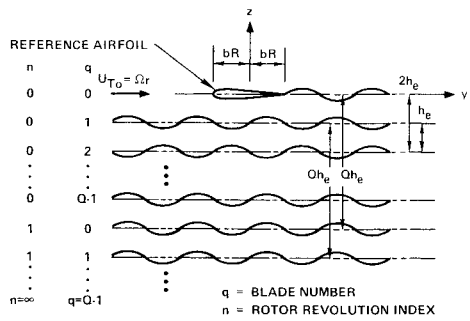

Fig. 1 Loewy's incompressible aerodynamic model.

by minimizing the modified function

$$\sum_{j=1}^{m} [C(k_j)D(ik_j) - N(ik_j)]^2$$

The [4,4] Padé approximant obtained for this case was found to be very good approximation to the lift deficiency function $C(k)$.

Dowell[10] used a different approach to obtain the approximate functional form of $C(k)$. First, he assumed the indicial response function for a two-dimensional airfoil in incompressible flow. Since Jones[6] derived an approximate functional form for Wagner's indicial lift function, given by

$$\phi_{FW}(\tau) \simeq 1.0 - 0.165e^{-0.0455\tau} - 0.335e^{-0.3\tau} \tag{7}$$

Dowell[10] assumed an indicial response function similar in form to Eq. (7):

$$\phi_{FW}(\tau) = \sum_{j=1}^{N} a_j e^{b_j\tau}, \qquad \tau \geq 0$$

$$= 0, \qquad \tau < 0 \tag{8}$$

For a stable or convergent indicial response function, b_j should be negative throughout.

The indicial response function is related to Theodorsen's lift deficiency function through a Fourier transform,[15] i.e.,

$$\phi_{FW}(\tau) = \frac{1}{2\pi}\int_{-\infty}^{\infty} \frac{C(k)}{ik} e^{ik\tau} dk \tag{9}$$

Taking the inverse transform of Eq. (9),

$$C(k) = ik\int_{-\infty}^{\infty} \phi_{FW}(\tau) e^{ik\tau} d\tau \tag{10}$$

Substituting Eq. (8) into Eq. (10) and integrating, $C(k)$ becomes

$$C(k) = \sum_{j=1}^{N} \frac{a_j ik}{(-b_j + ik)} \tag{11}$$

In Ref. 10, Dowell first selected b_j to be on the negative real axis, i.e., negative values for b_j, to account for a convergent $\phi_{FW}(\tau)$ given by Eq. (8). Subsequently, the coefficient a_j was determined. Using this procedure, Dowell obtained a very good approximation to Theodorsen's lift deficiency function $C(k)$. The main difference between Vepa's and Dowell's procedures is that Vepa directly assumed an approximate form for $C(k)$ in terms of a ratio of polynomials, whereas Dowell began by assuming the indicial response function and determined the a_j coefficients after assigning specific values to b_j. It should be noted that Dowell's procedure is based on the assumption that the functional form of the indicial response function *is known a priori*.

In Ref. 12, Dinyavari and Friedmann used Dowell's procedure to obtain the approximate transfer function for Loewy's lift deficiency function for the cross section of a helicopter blade. The poles of the transfer function were placed on the negative real axis in a manner consistent with Dowell's assumption of negative values for b_j. The a_j coefficients were thus determined. The approximate transfer function obtained in this manner failed to capture the oscillatory behavior of Loewy's lift deficiency function; thus, correlation between the approximate model and the exact value of Loewy's function was found to be poor. It is shown below that the Bode plot of aerodynamic transfer function provides the necessary information regarding the nature of the poles and zeros (such as real or complex) as well as their locations in the Laplace plane. This information can be used to formulate the approximate aerodynamic transfer functions in an accurate and reliable manner.

The Bode Plot and Its Role in Unsteady Aerodynamic Modeling

One of the methods frequently used in the analysis and design of control systems is the frequency response method. When using this method, the frequency of the input is varied over a wide range and the resulting output response is studied. Using this method, the transfer functions of complicated systems can be determined. This particular aspect of determining the transfer function from the frequency response curve can also be used to formulate approximate transfer functions for the unsteady aerodynamics of a two-dimensional airfoil oscillating in incompressible flow. Furthermore, the method is equally applicable to both fixed- or rotary-wing-type unsteady aerodynamic theories where the lift deficiency function plays essentially the role of a transfer function, which relates the ¾-chord downwash velocity to the aerodynamic load acting on the airfoil. Since the lift deficiency functions—such as Theodorsen's for the fixed-wing case and Loewy's for the rotary-wing case—are known exactly for simple harmonic motion of the airfoil, the approximate transfer functions can be formulated by the application of frequency response techniques used in control system engineering.

One of the methods used for representing the frequency response of a transfer function is the Bode diagram,[13] which consists of two parts. One is a plot of the logarithm of the magnitude of the sinuosidal transfer function, the other is a plot of the phase angle. Both are plotted as a function of frequency on a logarithmic scale. Since only the magnitude vs frequency plot is needed for the present application, the following discussion is restricted to this particular aspect of the Bode plot.

The standard representation of the Bode plot consists of a logarithmic magnitude of the transfer function $G(i\omega)$—i.e., 20 log $|G(i\omega)|$—vs the frequency ω.

Since the present aim is to formulate an approximate transfer function to the unsteady lift deficiency function, information about the qualitative nature of the poles and zeros, i.e., whether they are real or complex and where they are located, is sought. This information can be obtained by analyzing the Bode plot of the lift deficiency function. A detailed description of the features of the Bode plot and its asymptotic properties, which is useful for a more complete understanding of this paper, can be found in Refs. 13 and 16, and for the sake of conciseness is not repeated here. The most important properties of the Bode plots needed for the present application are summarized below:

1) A +20 dB/decade change in slope in the asymptotes is indicative of the presence of a real zero, and a −20 dB/decade change in slope indicates the presence of a real pole in the transfer function.

2) Peaks in the Bode plot indicate the presence of complex poles and complex zeros in the transfer function.

3) A −40 dB/decade change in slope in the asymptotes indicates the presence of either complex poles or two equal real

poles, and a +40 dB/decade change in slope indicates the presence of either complex zeros or two equal real zeros.

4) Whenever the slopes of asymptotes of the transfer function are equal, at low and high frequencies, the transfer function should have an equal number of poles and zeros.

These properties are directly applicable to the formulation of approximations to the lift deficiency function, which has the role of an aerodynamic transfer function in unsteady aerodynamics.

Finite-State Modeling of Theodorsen's Lift Deficiency Function

Theodorsen's lift deficiency function for a two-dimensional airfoil executing a simple harmonic motion in incompressible flow is given in exact form by[15]

$$C(k)=\frac{H_1^2(k)}{H_1^2(k)+iH_0^2(k)}=F+iG \tag{12}$$

The real and imaginary parts of $C(k)$ are shown in Fig. 2. Figure 3 shows the Bode plot of Theodorsen's lift deficiency function. It can be seen from Fig. 3 that the low- and high-frequency asymptotes have equal slopes with a value of 0 dB/decade. Also, the Bode plot does not show any peaks, and the slope of the exact curve at any point is less than −20 dB/decade. Therefore, using the general properties of the Bode plots presented previously, the approximate transfer function for $C(k)$ must have an equal number of poles and zeros. Furthermore, the poles and zeros should be real. Based on these considerations, a second-degree Padé approximation for $C(k)$ can be assumed in the following form:

$$C(k)\simeq\frac{0.5(ik+a_1)(ik+a_2)}{(ik+b_1)(ik+b_2)} \tag{13}$$

The transfer function satisfies the condition that $C(k)$ approaches 0.5 as k approaches infinity. Imposing the constraint that $C(k)=1$ for $k=0$, the coefficients a_1, a_2, b_1, b_2 are determined by a least-squares technique by equating the real and imaginary parts of the transfer function with the real and imaginary parts of the exact function $C(k)$. The approximate function obtained in this manner is given by

$$C(k)=\frac{0.5(ik+0.135)(ik+0.651)}{(ik+0.0965)(ik+0.4555)} \tag{14}$$

The real and imaginary parts of the approximate transfer function are shown in Fig. 2 along with the exact functions. It can be seen that the approximate function deviates slightly from the exact function in the frequency range $0.05\leq k\leq 0.5$. For the sake of comparison, Jones' approximation to Theodorsen's function $C(k)$ is also plotted in Fig. 2.

The location of the poles (P_1,P_2) and zeros (Z_1,Z_2) and the asymptotic behavior of the approximate function, given in Eq. (14), are shown in Fig. 3. At very low frequencies, the slope of the asymptote is 0 dB/decade and the asymptote is the 0 dB line. At pole $P_1=-0.0965$, the slope of the asymptote becomes −20 dB/decade. The transfer function has a zero at $Z_1=0.135$ and, hence, there is a change of slope of +20 dB/decade. The combined effects of the pole P_1 and zero Z_1 cause the slope of the asymptote at Z_1 to be 0 dB/decade, which is indicated by the line Z_1P_2. At point P_2, the function has a pole $P_2=-0.4555$ and the slope of the asymptote becomes −20 dB/decade. At point Z_2, where there is a zero, $Z_2=-0.651$, the slope of the asymptote again reverts back to 0 dB/decade.

By including an additional pole and zero in the transfer function given in Eq. (13), a third-degree [3,3] Padé approx-

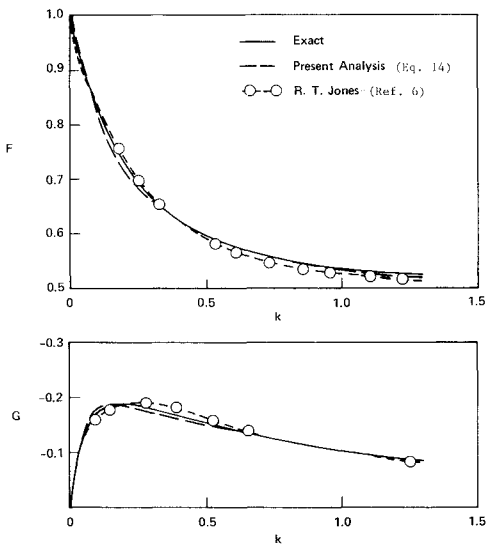

Fig. 2 Theodorsen's lift deficiency function.

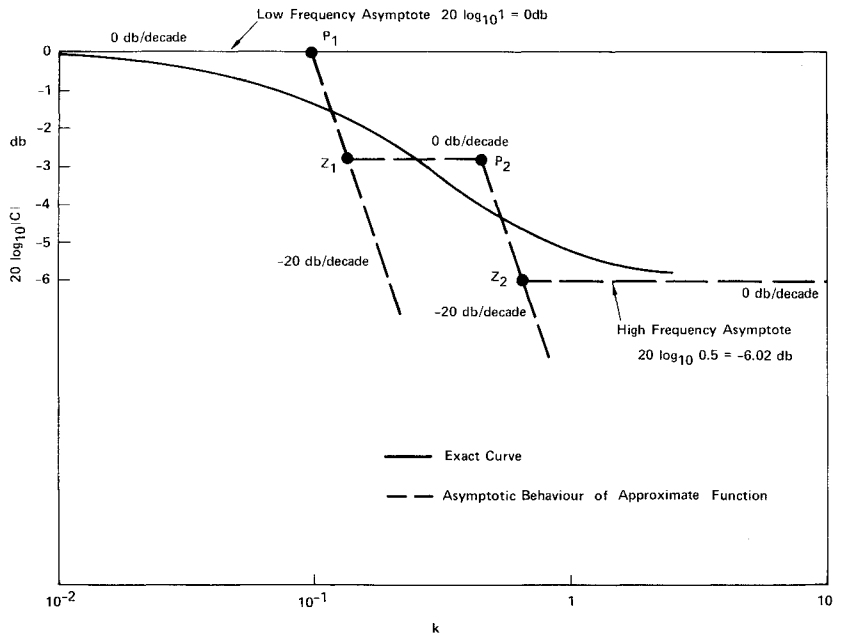

Fig. 3 Bode plot of Theodorsen's lift deficiency function, 2-pole approximation.

imation for Theodorsen's lift deficiency function is obtained. After including the effect of the additional pole and zero, the approximate transfer function is given by

$$C(k) \simeq \frac{0.5(ik+0.088)(ik+0.37)(ik+0.922)}{(ik+0.072)(ik+0.261)(ik+0.80)} \tag{15}$$

The real and imaginary parts of the exact $C(k)$ function together with the approximate transfer function, given in Eq. (18), are shown in Fig. 4. It is evident that the [3,3] Padé approximation gives excellent correlation with the exact $C(k)$ functions. The location of the poles and zeros and the asymptotic behavior of the approximate transfer function, given in Eq. (15), are shown in Fig. 5. It can be seen from Figs. 5 and 3 that the poles and zeros of the approximate transfer function lie in the range of k where the Bode plot of the exact transfer function has a higher slope than at other values of k, i.e., $0.06 \leq k \leq 1.0$. This particular feature, which is associated with the location of the poles and zeros, is very useful for estimating their initial values. This is an important ingredient when constructing the approximate transfer function using a nonlinear least-squares technique.

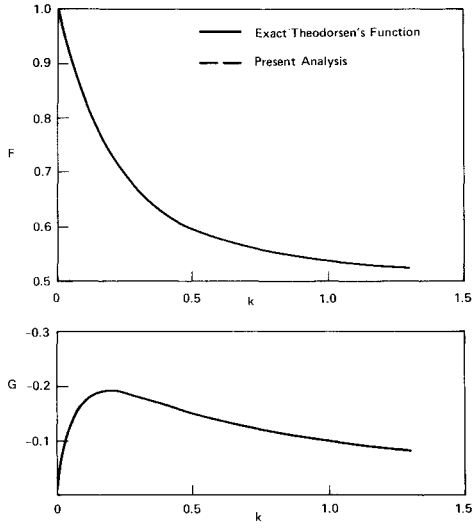

Fig. 4 Theodorsen's lift deficiency function, 3-pole approximation [Eq. (15)] (two curves coincide).

The indicial response function can be obtained by taking the inverse Fourier transform of the approximate transfer function, which has been obtained above. Using the [2,2] Padé approximation, given by Eq. (14), the indicial response function is

$$\phi_{FW}(\tau) \simeq 1.0 - 0.309e^{-0.0965\tau} - 0.191e^{-0.4555\tau} \tag{16}$$

Jones'[6] approximation to Wagner's indicial response function is

$$\phi_{FW}(\tau) \simeq 1.0 - 0.165e^{-0.0455\tau} - 0.335e^{-0.3\tau} \tag{17}$$

Comparing these two indicial response functions, it can be seen that the indicial response obtained herein has a smaller time constant when compared to those in Jones' approximation.

The indicial response function obtained for the [3,3] Padé approximation, given by Eq. (15), is

$$\phi_{FW}(\tau) \simeq 1.0 - 0.203e^{-0.072\tau} - 0.236e^{-0.261\tau} - 0.06e^{-0.8\tau} \tag{18}$$

Finite-State Modeling of Loewy's Lift Deficiency Function

The procedure described in the preceding section for constructing approximations to Theodorsen's lift deficiency function is also applicable to the formulation of approximations to Loewy's lift deficiency function, which is the rotary-wing counterpart of Theodorsen's theory. Loewy's rotary-wing, unsteady airfoil theory represents an approximation to the unsteady aerodynamic loads acting on a rotor-blade cross section *in hover*. The effects of the spiral returning wake beneath the rotor, shown in Fig. 1, are considered in an approximate manner. These wake layers represent wakes shed by other blades, as well as the reference blade in previous revolutions. The approximation consists of the assumption that the wake layers extend to infinity before and behind the reference airfoil. Loewy's theory is intended for lightly loaded rotors—i.e., low inflow conditions—and, similar to Theodorsen's theory, is also based on the assumption of simple harmonic motion of the reference airoil.

Loewy's lift deficiency function in the frequency domain for the *collective mode* of the rotor, where all of the blades move in phase, is given by[11]

$$C'(k,\bar{m}_e,\bar{h}_e) = H_1^2(k) + 2J_1(k)W(k\bar{h}_e,\bar{m}_e)$$
$$\div H_1^2(k) + iH_0^2(k) + 2[J_1(k) + iJ_0(k)]W(k\bar{h}_e,\bar{m}_e) \tag{19}$$

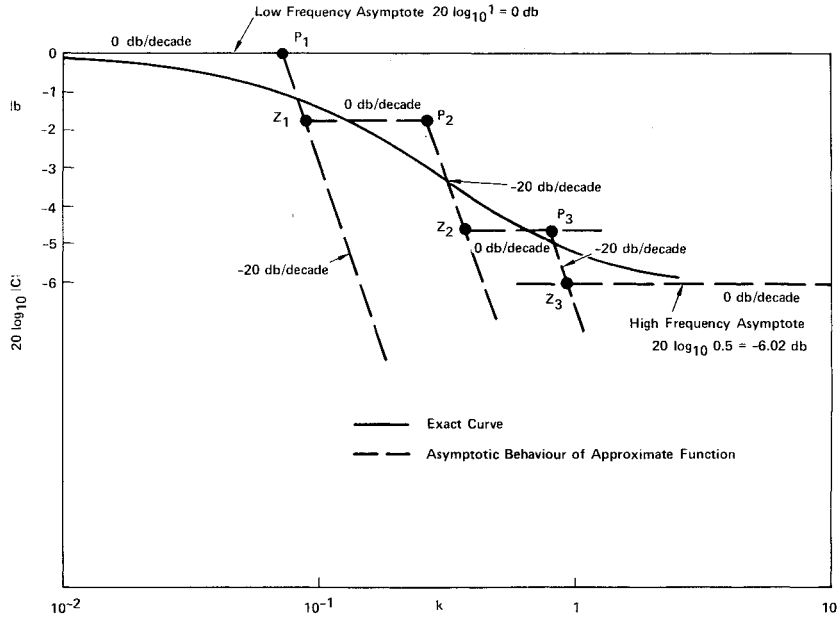

Fig. 5 Bode plot of Theodorsen's lift deficiency function, 3-pole approximation, [Eq. (15)].

where the wake weighting function W is

$$W(k\bar{h}_e, \bar{m}_e) = \frac{1}{e^{k\bar{h}_e e^{i2\pi\bar{m}_e - 1}}}, \qquad k > 0$$

$$= 0, \qquad k = 0 \tag{20}$$

The quantities $\bar{h}_e$ and $\bar{m}_e$ for a typical blade section at a radial distance r from the axis of rotation for a rotor with Q blades are defined as

$$\bar{m}_e = \frac{\omega}{\Omega Q} = \frac{\omega b}{\Omega r} \cdot \frac{r}{Qb} = k\bar{r}_e; \quad \bar{r}_e = \frac{r}{Qb}$$

$$\bar{h}_e = \frac{2\pi U_{p0}}{\Omega Q b} = \frac{2\pi U_{p0}}{\Omega R} \frac{R}{Qb} = \frac{2\pi\lambda_0}{Q(b/r)}$$

In the definition of the equivalent frequency ratio $\bar{m}_e$, it should be noted that for a given blade section at a radial station r from the axis of rotation, $\bar{m}_e$ depends on the reduced frequency k.

It will be shown that the technique based on the Bode plot developed herein is successful in formulating the approximate transfer function for Loewy's lift deficiency function. To illustrate the method, two examples were selected. Example 1 is the same as that considered in Ref. 12, with $\bar{h}_e = 4.0$ and $\bar{r}_e = 3.0$. This case corresponds to a blade section located at a radial station $0.8R$. The rotor consists of four blades with a blade semichord $b/R = 0.0667$. The rotor is operating at a thrust coefficient $C_T = 0.058$, and the corresponding inflow ratio is $\lambda_0 = (C_T/2)^{1/2} = 0.17$. These values of C_T and λ_0 are unreasonably high for a helicopter; however, this case was selected to test the method for an extreme case. For example 2, $C_T = 0.005$ and the blade section was taken at $0.75R$. The rotor consists of four blades, and the blade semichord is $b/R = 0.024$. The inflow ratio is $\lambda_0 = (C_T/2)^{1/2} = 0.05$. The corresponding values of $\bar{h}_e$ and $\bar{r}_e$ are $\bar{h}_e = 3.2725$ and $\bar{r}_e = 7.8125$. This example is representative of a typical helicopter application.

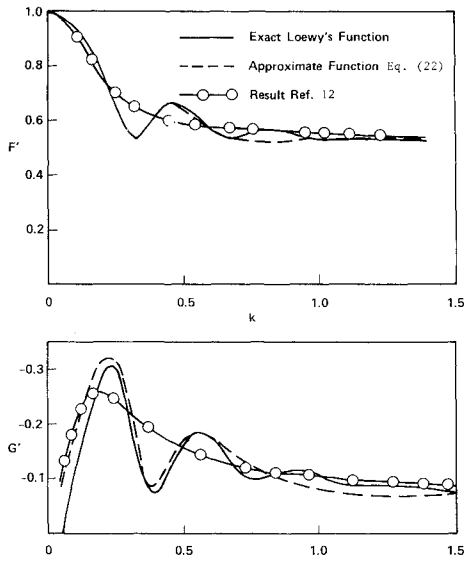

Fig. 6 Loewy's lift deficiency function and its approximation for example 1.

Example 1

The prescribed parameters for example 1 are: $\bar{h}_e = 4.0$, $\bar{r}_e = 3.0$, $Q = 4$, and $C_T = 0.058$ (Ref. 12). The real and imaginary parts of Loewy's exact lift deficiency function C' are shown in Fig. 6. Both the real (F') and imaginary (G') parts of Loewy's lift deficiency function exhibit an oscillatory behavior. Also shown in Fig. 6 is the approximate lift deficiency function obtained in Ref. 12 by using a [5,5] Padé approximant. The agreement between this approximation and the exact values of Loewy's lift deficiency function is poor. Figure 7 shows the Bode plot of the Loewy's lift deficiency function C'. This log-frequency curve exhibits peaks and valleys. As mentioned previously, the presence of peaks and valleys in the Bode plot is indicative of complex poles and complex zeros in the transfer function. Therefore, the approximate transfer function for C' must have complex poles and complex zeros. Based on this requirement, the approximate transfer function selected for C' is of the form

$$C'(k, \bar{m}_e, \bar{h}_e) \simeq \frac{0.5(ik + a_1)[(ik)^2 + ika_2 + a_3][(ik)^2 + ika_4 + a_5]}{(ik + b_1)[(ik)^2 + ikb_2 + b_3][(ik)^2 + ikb_4 + b_5]} \tag{21}$$

The approximate transfer function given in Eq. (21) satisfies the high-frequency limit, therefore, when k approaches ∞, C'

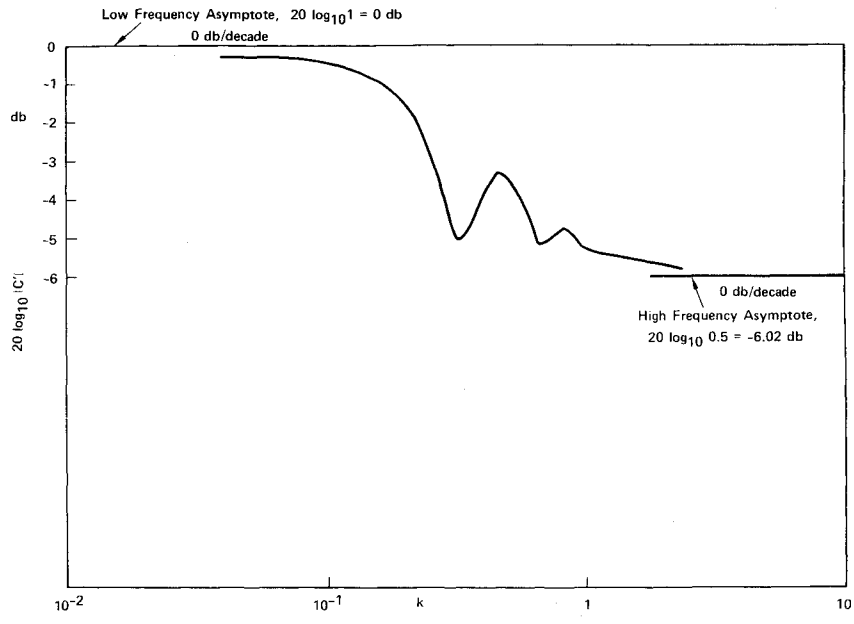

Fig. 7 Bode plot of Loewy's lift deficiency function for example 1.

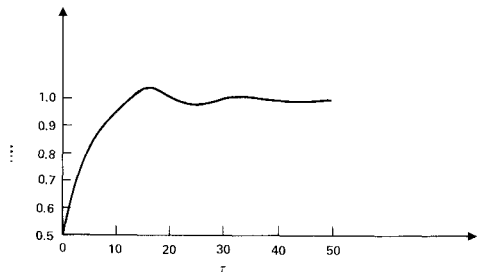

Fig. 8 Rotary-wing indicial response function for example 1.

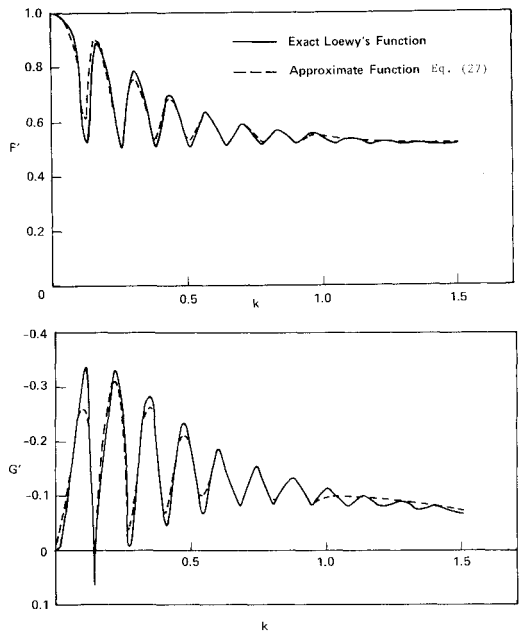

Fig. 9 Loewy's lift deficiency function and its approximation for example 2.

approaches 0.50. The approximate function, given by Eq. (21), is capable of representing the complex poles and complex zeros, depending on the values of the coefficients b_2, b_3, b_4, b_5 and a_2, a_3, a_4, a_5. Since the values of the exact Loewy lift deficiency function C' are known at various reduced frequencies k, the coefficients $a_1,\ldots,a_5$ and $b_1,\ldots,b_5$ can be evaluated. In this case, the coefficients are evaluated using a nonlinear least-squares technique based on the Fletcher-Powell algorithm. After evaluating the coefficients, the approximate transfer function or lift deficiency function becomes

$$C' = F' + iG' \simeq \{0.5(ik+1.153)[(ik)^2+0.131ik+0.119] \times [(ik)^2+0.623ik+0.53]\}/\{(ik+0.485)[(ik)^2+0.202ik+0.133][(ik)^2+0.893ik+0.561]\} \quad (22)$$

In Fig. 6, the real and imaginary parts of the approximate lift deficiency function, given by Eq. (22), are plotted together with the exact values of F' and G'. It can be seen from Fig. 6 that the approximate transfer function reproduces exactly the oscillatory nature of Loewy's lift deficiency function. From Fig. 6, it is evident that both the real and imaginary parts of the approximation to Loewy's lift deficiency function deviate from the exact values for $k > 0.70$. The important item to note, however, is the ability of the approximate function to capture the oscillatory behavior of the exact function. In this case, the approximation obtained is much better than that obtained in Ref. 12, with the same [5,5] order Padé approximation for the transfer function. Even better approximations could be obtained by adding additional poles and zeros to the transfer function given in Eq. (21).

Table 1 Poles and zeros of the approximate transfer function used in example 2; $C' \simeq N(ik)/D(ik)$ [Eq. (27)]

Poles	Zeros
Roots of $D(ik)$	Roots of $N(ik)$
$-0.0200 \pm i0.1293$	$-0.0138 \pm i0.1254$
$-0.0276 \pm i0.2617$	$-0.0183 \pm i0.2574$
$-0.0295 \pm i0.3859$	$-0.0212 \pm i0.3847$
$-0.0357 \pm i0.5127$	$-0.0259 \pm i0.5085$
$-0.0382 \pm i0.6293$	$-0.0344 \pm i0.6509$
$-0.0489 \pm i0.7558$	$-0.0511 \pm i0.7351$
$-0.0581 \pm i0.8262$	$-0.0655 \pm i0.8459$
$-0.0487 \pm i0.9259$	$-0.0445 \pm i0.9153$
-0.2549	-0.5691

It can be seen from Eq. (22) that the roots of the second and third terms in both the numerator and denominator are complex roots, indicating that the transfer function has complex zeros and poles. The complex poles are $-0.101 \pm i0.351$ and $-0.4465 \pm i0.601$, respectively, while the complex zeros are $-0.0655 \pm i0.339$ and $-0.312 \pm i0.658$. The presence of these complex poles and zeros is indicated by the peaks and valleys in the Bode plot for Loewy's exact lift deficiency function.

An important aspect of the oscillatory behavior of Loewy's lift deficiency function is considered next. From linear, incompressible, two-dimensional, unsteady aerodynamic theory for fixed wings, it can be proven mathematically that Wagner's indicial response function and Theodorsen's lift deficiency function are related by a Fourier transform.[15] Since Loewy's theory is the rotary-wing counterpart of Theodorsen's theory, it is evident by analogy that the rotary-wing indicial response function and Loewy's lift deficiency function can also be related by a Fourier transform. Thus, the rotary-wing indicial response function can be obtained from the following relation:

$$\phi_{RW}(\tau) = \tfrac{1}{2}\pi \int_{-\infty}^{\infty} \frac{C'(ik)}{ik} e^{ik\tau} dk \quad (23)$$

The approximate transfer funciton, given in Eq. (22), can be substituted in Eq. (23) for C'. Applying partial fractions and using a table of inverse Laplace transforms, the approximate rotary-wing indicial response function can be obtained. In this case, the approximate indicial response function is given by

$$\phi_{RW}(\tau) \simeq 1.0 - 0.942e^{-0.485\tau} + e^{-0.101\tau}(0.177\cos 0.351\tau - 0.073\sin 0.351\tau) + e^{-0.446\tau}(0.264\cos 0.601\tau - 0.22\sin 0.601\tau) \quad (24)$$

The indicial response function $\phi_{RW}(\tau)$ is plotted in Fig. 8, where it can be seen that the indicial response is oscillatory and, at certain values of τ, the response overshoots the steady value of 1.0. This result indicates that, for a step change in angle of attack of the rotor blade, the thrust developed by the rotor will overshoot the steady value before finally reaching the steady value. This phenomenon has been experimentally observed by Carpenter and Fridovitch,[14] who noted that for a rapid change in collective pitch setting of a model rotor, the measured thrust overshoots the steady value of the thrust. This is precisely the trend evident from the indicial response function $\phi_{RW}(\tau)$ given by Eq. (24) and shown in Fig. 8. Furthermore, it should be noted that this is the first time that a rotary-wing indicial response function has been presented in the literature.

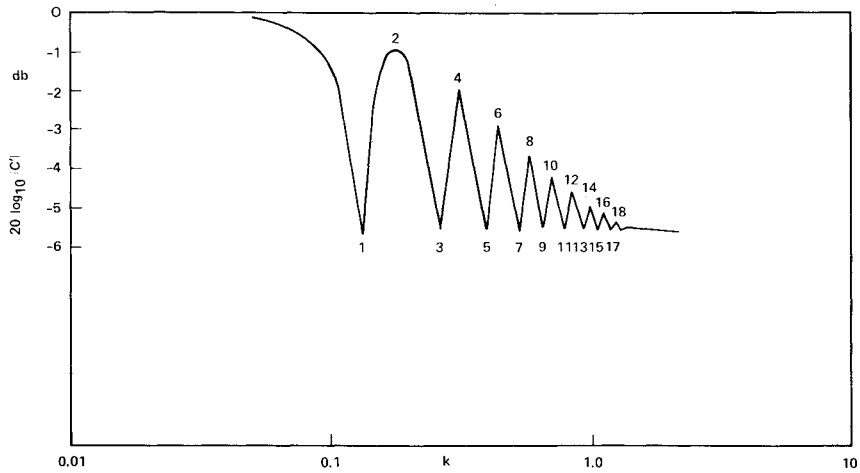

Fig. 10 Bode plot of Loewy's lift deficiency function for example 2.

In general, the rotary-wing indicial response function can be written as

$$\phi_{RW}(\tau) \simeq 1.0 - \sum_{j=1}^{N} e^{-b_j\tau}[A_j \cos\omega_j\tau + B_j \sin\omega_j\tau] \tag{25}$$

The values of A_j, B_j, and b_j depend on the rotor geometry and rotor operating conditions. They can be evaluated from the approximate transfer function corresponding to Loewy's lift deficiency function defined for that specific rotor.

Recall from the previous discussion of the fixed-wing case that the indicial response function can be written as

$$\phi_{FW}(\tau) \simeq 1.0 - \sum_{j=1}^{N} A_j e^{-b_j\tau} \tag{26}$$

Comparing the rotary-wing indicial response functions ϕ_{RW} [Eq. (25)], with the fixed-wing indicial response function ϕ_{FW} [Eq. (26)], it can be concluded that the rotary-wing indicial response function is qualitatively different from the fixed-wing indicial response function; the former exhibits an oscillatory nature, whereas the latter is nonoscillatory.

Example 2

The prescribed parameters for example 2 are: $\bar{h}_e = 3.2725$, $\bar{r}_e = 7.8125$, $Q = 4$, and $C_T = 0.005$. The location of the typical blade section is selected to be at $0.75R$. The blade semichord is $b/R = 0.024$.

Figure 9 illustrates the real (F') and imaginary (G') parts of Loewy's exact lift deficiency function for the values of $\bar{h}_e = 3.2725$ and $\bar{r}_e = 7.8125$. The real and imaginary parts of Loewy's lift deficiency function are highly oscillatory. The Bode plot of Loewy's lift deficiency funciton is presented in Fig. 10. The Bode plot has many peaks and valleys. Hence, the corresponding approximate lift deficiency or transfer function sought must have as many complex poles and complex zeros as there are peaks and valleys in the Bode plot. In Fig. 10, the odd numbers—which correspond to the valleys—indicate complex zeros, and the even numbers—corresponding to the peaks—indicate complex poles. For practical situations, high reduced frequencies above $k \geq 1$ are not common in rotary-wing applications. Therefore, in this case, the approximate transfer function is constructed to capture the first eight complex poles and complex zeros. This approximate transfer function can be written in the following form:

$$C'(k, \bar{h}_e, \bar{m}_e) = F' + G' \simeq \frac{0.5(ik + a_1)}{(ik + b_1)} \times \frac{\prod_{j=1}^{8} [(ik)^2 + a_{2j} ik + a_{2j+1}]}{\prod_{j=1}^{8} [(ik)^2 + b_{2j} ik + b_{2j+1}]} \tag{27}$$

Table 1 gives all the poles and zeros of the approximate transfer function represented by Eq. (27). It can be seen that there are eight complex poles and eight complex zeros, in addition to one real pole and a real zero. The details of the calculations of the poles and zeros are given in Ref. 16.

In Fig. 9, the real and imaginary parts of the approximate lift deficiency or transfer function are shown together with Loewy's exact lift deficiency function. It can be seen that the approximate transfer function follows Loewy's exact lift deficiency function, and the agreement between the two curves is very good. The indicial response function obtained using this approximate transfer function[16] overshoots the steady value of the response at certain values of time τ, and the indicial response function is qualitatively similar to the indicial response function obtained for the first example shown in Fig. 8.

Finally, it should be noted that Loewy's lift deficiency function was used in its original form herein. However, it has been shown in Refs. 17 and 18 that the zero-frequency limit of Loewy's lift deficiency function does not approach unity as the reduced frequency approaches zero.

Concluding Remarks

In unsteady aerodynamic theories, the lift deficiency function plays the role of an aerodynamic transfer function relating the ¾-chord downwash velocity to the lift on the airfoil. Therefore, the Bode plot of the lift deficiency function can be used to obtain important information regarding the qualitative nature of the poles and zeros as well as their locations. Using this information, approximate finite-state lift deficiency functions were formulated successfully for both fixed- and rotary-wing applications, such as Theodorsen's and Loewy's lift deficiency functions.

Based on the approximate transfer function obtained for the lift deficiency functions, the indicial response functions were evaluated. It was found that the rotary-wing indicial response function has an oscillatory nature, which causes the indicial response to overshoot its steady-state value before reaching it. This behavior is also consistent with experimental evidence.[14] On the other hand, the fixed-wing indicial response is nonoscillatory. Furthermore, it should be emphasized that this is the first time that a rotary-wing indicial response function has been presented in the literature.

The finite-state, unsteady aerodynamic model obtained in the present study has a number of important potential applications in rotary-wing aeroelastic stability and response studies, such as: 1) rotary-wing aeroelastic stability and response problems in forward flight, 2) simulation of subcritical flutter testing of rotors where the determination of damping levels is important before actual flutter boundaries are encountered, and 3) treatment of rotary-wing aeroelastic systems with active feed-back control systems, such as higher harmonic controls.

Finally, it should be noted that the present study should be viewed as a contribution to the much broader field of unsteady airfoils, which has been reviewed in detail in Ref. 19.

Acknowledgments

This study was supported by NASA Ames Research Center under Grant NASA NAG 2-209. The authors would like to thank Mr. V. Ramanarayanan of the California Institute of Technology for discussions regarding the modeling of transfer functions based on the Bode plot.

References

[1]Theodorsen, T., "General Theory of Aerodynamic Instability and the Mechanism of Flutter," NACA Rept. 496, 1935.

[2]Greenberg, J. M., "Airfoil in Sinusoidal Motion in Pulsating Stream," NACA TN 1326, 1947.

[3]Loewy, R. G., "A Two-Dimensional Approximation of Unsteady Aerodynamics of Rotary Wings," *Journal of the Aeronautical Sciences*, Vol. 24, No. 2, Feb. 1957. pp. 81-92,144.

[4]Shipman, K. W. and Wood, E. R., "A Two-Dimensional Theory for Rotor Blade Flutter in Forward Flight," *Journal of Aircraft*, Vol. 8, Dec. 1971, pp. 1008-1015.

[5]Garrick, G. E., "On Some Reciprocal Relations in the Theory of Non-stationary Flows," NACA Rept. 629, 1938.

[6]Jones, R. T., "The Unsteady Lift of a Wing of Finite Aspect Ratio," NACA Rept. 681, 1940.

[7]Sears, W. R., "Operational Methods in the Theory of Airfoils in Non-uniform Motion," *Journal of the Franklin Institute*, Vol. 230, No. 1, July 1940.

[8]Edwards, J. W., "Unsteady Aerodynamic Modelling and Active Aeroelastic Control," Stanford University, CA, SUDAAR 504, Feb. 1977.

[9]Vepa, R., "On the Use of Padé Approximants to Represent Unsteady Aerodynamic Loads for Arbitrary Small Motions of Wings," AIAA Paper 76-17, Jan. 1976.

[10]Dowell, E. H., "A Simple Method for Converting Frequency Domain Aerodynamics to the Time Domain," NASA TM 81844, 1980.

[11]Johnson, W., *Helicopter Theory*, Princeton University Press, Princeton, NJ, 1980.

[12]Dinyavari, M.A.H. and Friedmann, P. P., "Unsteady Aerodynamics in Time and Frequency Domains for Finite Time Arbitrary Motion of Rotary Wings in Hover and Forward Flight," *Proceedings of the AIAA/ASME/ASCE/AHS 25th Structures, Structural Dynamics and Materials Conference*, Palm Springs, CA, May 1984, pp. 266-282.

[13]Ogata, K., *Modern Control Engineering*, Prentice-Hall, Englewood Cliffs, NJ, 1970.

[14]Carpenter, P. J. and Fridovitch, B., "Effect of Rapid Blade-Pitch Increase on the Thrust and Induced-Velocity Response of a Full Scale Helicopter," NACA TN 3044, Nov. 1953.

[15]Bisplinghoff, R. L., Ashley, H., and Halfman, R. L., *Aeroelasticity*, Addison-Wesley, Reading, MA, 1955.

[16]Venkatesan, C. and Friedmann, P. P., "Finite State Modelling of Unsteady Aerodynamics and Its Application to a Rotor Dynamic Problem," University of California, Los Angeles, CA, School of Engineering and Applied Science Report, UCLA-ENG-85-10, March 1985.

[17]Dinyavari, M. A. H., "Unsteady Aerodynamics in the Time and Frequency Domains for Finite-Time Arbitrary-Motion of Helicopter Rotor Blades in Hover and in Forward Flight," Ph.D. Dissertation, Mechanical, Aerospace, and Nuclear Engineering Department, University of California, Los Angeles, CA, March 1985.

[18]Dinyavari, M. A. H. and Friedmann, P. P., "Finite-Time Arbitrary-Motion Unsteady Cascade Airfoil Theory for Helicopter Rotors in Hover," *Proceedings of the Eleventh European Rotorcraft Forum*, Paper 26, London, England, Sept. 1985, pp. 26.1-26.32.

[19]McCroskey, W. J., "Unsteady Airfoils," *Annual Review of Fluid Mechanics*, Vol. 14, 1982, pp. 285-311.